

Widefield heterodyne interferometry using a custom CMOS modulated light camera

Rikesh Patel,* Samuel Achamfuo-Yeboah, Roger Light, and Matt Clark

*Applied Optics Group, Electrical Systems and Optics Research Division
University of Nottingham, University Park, Nottingham, NG7 2RD, UK*

*expr4@nottingham.ac.uk

Abstract: In this paper a method of taking widefield heterodyne interferograms using a prototype modulated light camera is described. This custom CMOS modulated light camera (MLC) uses analogue quadrature demodulation at each pixel to output the phase and amplitude of the modulated light as DC voltages. The heterodyne interference fringe patterns are generated using an acousto-optical frequency shifter (AOFS) in an arm of a Mach-Zehnder interferometer. Widefield images of fringe patterns acquired using the prototype MLC are presented. The phase can be measured to an accuracy of $\pm 6.6^\circ$. The added value of this method to acquire widefield images are discussed along with the advantages.

© 2011 Optical Society of America

OCIS codes: (100.3175) Interferometric imaging; (110.3175) Interferometric imaging.

References and links

1. N. A. Riza and M. A. Arain, "Angstrom-range optical path-length measurement with a high-speed scanning heterodyne optical interferometer," *Appl. Opt.* **42**, 2341–2345 (2003).
2. V. Ganapathi, C. Plagemann, D. Koller and S. Thrun, "Real time motion capture using a single time-of-flight camera," *Proc. IEEE Comput. Sci. Conf. on Comput. Vision Pattern Recognit.*, 755–762 (2010).
3. D. Droschel, D. Holzand, S. Behnke, "Multi-frequency phase unwrapping for time-of-flight cameras," *IEEE/RSJ 2010 Int. Conf. Intell. Rob. Syst.* **66**, 1463–1469 (2010).
4. X. Luan, R. Schwarte, Z. Zhang, Z. Xu, H.G. Heinol, B. Buxbaum, T. Ringbeck, and H. He, "3D intelligent sensing based on the PMD technology," *Proc. SPIE* **4540**, 482–487 (2001).
5. R. Onodera and Y. Ishii, "Two-wavelength laser-diode heterodyne interferometry with one phasemeter," *Opt. Lett.* **20**, 2502–2502 (1995).
6. S. Yokoyama, J. Ohnishi, S. Iwasaki, K. Seta, H. Matsumoto, and N. Suzuki, "Real-time and high-resolution absolute-distance measurement using a two-wavelength superheterodyne interferometer," *Meas. Sci. Technol.* **10**, 1233 (1999).
7. S. Vergamota, L. Cupido, M. Manso, F. Eusebio, A. Silva, P. Varela, J. Cabral, F. Serra, and C. Varandas, "Microwave interferometer with a differential quadrature phase detection," *Rev. Sci. Instrum.* **66**, 2547–2547 (1995).
8. H.-K. Teng and K.-C. Lang, "Heterodyne interferometer for displacement measurement with amplitude quadrature and noise suppression," *Opt. Commun.* **280**, 16–22 (2007).
9. S. Chamberlain and J. Lee, "Novel wide dynamic range silicon photodetector and linear imaging array," *IEEE J. Solid State Circuits* **20**, 41–48 (1984).
10. F. G. Cervantes, G. Heinzel, A. F. G. Marin, V. Wand, F. Steier, O. Jennrich, and K. Danzmann, "Real-time phase-front detector for heterodyne interferometers," *Appl. Opt.* **46**, 4541–4548 (2007).
11. A. Kimachi, "Real-time heterodyne imaging interferometry: Focal-plane amplitude and phase demodulation using a three-phase correlation image sensor," *Appl. Opt.* **46**, 87–94 (2007).
12. A. Kimachi, "Real-time heterodyne speckle pattern interferometry using the correlation image sensor," *Appl. Opt.* **49**, 6808–6815 (2010).

13. P. Dmochowski, B. Hayes-Gill, M. Clark, J. Crowe, M. Somekh, and S. Morgan, "Camera pixel for coherent detection of modulated light," *Electron. Lett.* **40**, 1403–1404 (2004).
 14. D. Summers, M. Clark, I. Stockford, S. Achamfuio-Yeboah, and J. Pereira Do Carmo, "Modulated light camera for space applications and assessment via a test bench system," *Acta Astronaut.* **66**, 1399–1403 (2010).
 15. M. Pitter, R. Light, M. Somekh, M. Clark, and B. Hayes-Gill, "Dual-phase synchronous light detection with 64 x 64 CMOS modulated light camera," *Electron. Lett.* **40**, 1404–1406 (2004).
 16. N. Johnston, C. Stewart, R. Light, B. Hayes-Gill, M. Somekh, S. Morgan, J. Sambles, and M. Pitter, "Quad-phase synchronous light detection with 64 x 64 CMOS modulated light camera," *Electron. Lett.* **45**, 1090–1092 (2009).
-

1. Introduction

Interferometry is used in a wide variety of fields for instrumentation and analysis of subjects and the environment. This paper describes a method for creating a widefield image of heterodyne interference patterns, using a custom CMOS modulated light camera. Interference of light occurs when two beams are superimposed upon each other. Widefield interference patterns captured can be used to determine any change in the optical path length of these two beams across a 2D area. The camera presented measures phase in modulated light generated by heterodyne interference, which is much less susceptible to optical noise when compared with a system detecting homodyne interference. It is capable of continuous pixel reads, outputting both intensity and phase data simultaneously, and demodulate light in the megahertz region.

Homodyne interferometry happens when both beams have the same frequency. This will create interference patterns with intensity that will not change with time and only with optical path length difference in the interferometer. The intensity measured using this technique is susceptible to many forms of noise which could include contributions from background light, electrical noise, mechanical vibrations and crucially if those noise sources are faster than the detector response.

Heterodyne interferometry uses beams with different frequencies, resulting in AC interference patterns at the difference between the frequencies, also known as the beat frequency. When interference occurs, the phase difference between the two light beams is no longer static. The interference pattern intensity is modulated at the beat frequency.

Although it is not straightforward to bring into practice a widefield heterodyne system, the benefit of using a heterodyne over a homodyne interferometer is that the system is much less susceptible to noise. Any constant additional background intensity or low frequency optical noise will have a major effect on any homodyne system unless the effect is calibrated for, which could be difficult. Random noise introduced into the system would also be difficult to remove, especially so with single point detection. Scanning techniques have been used [1], however, for real time applications this becomes more of a challenge, especially if the phase change induced by a subject is time variant.

Using the heterodyne interferometer described in this paper, many noise components are filtered or mixed out which should result in better noise characteristics when compared with a homodyne system. Phase information is extracted without complex processing of intensity [2,3] or phase stepping using multiple frames or cameras [4]. With one light source and an integrated camera, compact systems can be designed, which should be more beneficial in both industry and research settings.

In work previously conducted, heterodyne interference was detected using a point detector. Fringe patterns were largely ignored in favour of detecting a single phase output. In this situation, data involving subjects where phase changed differently across the area of analysis was lost. Onodera and Ishii produced work that used phasemeters [5] to determine point phases from the output of a heterodyne interferometer, with Riza and Arain, and Yokoyama et al. developing a system that is high in precision [1, 6]. Much like the work in this paper, Vegamota et al. and Teng and Lang used quadrature demodulation to produce phase information [7,8], however, this

was again done using one measuring sensor. Widefield heterodyne detection systems developed have been able to detect a single point on an interference pattern with 2D images produced by scanning across a pattern [1] presented by Riza and Arain and a system which uses a CCD camera [10] presented by Cervantes et al. Despite being able to measure at high precision, the equipment used to generate different frequency light is expensive and methods of alignment are difficult. Scanning systems, for real time applications, become more of a challenge, especially if the phase change induced by a subject is time variant and with CCD cameras, it becomes difficult to work at high modulation frequencies with modulation frequency of up to 10kHz being detected.

Kimachi has developed a system using a three phase correlation sensor which contains an array of CMOS pixels of 64x64 [11] and more recently 200x200 [12]. The system is reported to work with a beat frequency of 25kHz and is able to produce 30 frames/s. However, this type of camera uses signal bins in the form of capacitors. This holds the charge transferred from the photodiode. The integration time determines how often the pixels can be read as well the maximum beat frequency than can be used with the system.

The method and instrumentation described in this paper is used to create a real time wide-field image of a heterodyne interference pattern. This uses the custom CMOS modulated light camera (MLC) described in this paper, which does not use signal bins and allows pixel data to be accessed readily with no dead time between readings [13]. This allows for the systems to be based around much higher beat frequencies with the ability to minimise read errors through multiple reads and averaging. The light modulation frequency detected using the prototype MLC is 15MHz, produced with a modified Mach-Zehnder interferometer using a Bragg Cell in one arm.

2. Optical arrangement

The interferometer setup described in this paper is based on a Mach-Zehnder design. In a standard Mach-Zehnder interferometer, a light beam is split using a beam splitter then interfered using another beam splitter. In our system, as can be seen in Fig. 1, one arm of the interferometer is passed through an acousto-optic frequency shifter (AOFS). This device will shift the frequency of incoming light by 15MHz. The resultant interference pattern is modulated at that frequency. The heterodyne interference pattern can be described mathematically by considering the real part of the beams in scalar form, $E_R(x, y, t)$ and $E_I(x, y, t)$, by,

$$\begin{aligned} E_R(x, y, t) &= a_r(x, y) \cos(2\pi f_r t + \phi_r(x, y)) \\ E_I(x, y, t) &= a_i(x, y) \cos(2\pi f_i t + \phi_i(x, y)) \end{aligned} \quad (1)$$

In these equations, the waves travel in the same direction but have different frequencies, f and phase, ϕ . Time and amplitude are represented by t and a respectively. When interference occurs, the intensity of the sum of these two wavefronts, $I(x, y, t)$, can be expressed by,

$$\begin{aligned} I(x, y, t) &= [E_R(x, y, t) + E_I(x, y, t)]^2 \\ &= \frac{1}{2} a_r(x, y)^2 + \frac{1}{2} a_i(x, y)^2 + \frac{1}{2} a_r(x, y)^2 \cos(2\omega_r t + 2\phi_r(x, y)) \\ &\quad + \frac{1}{2} a_i(x, y)^2 \cos(2\omega_i t + 2\phi_i(x, y)) \\ &\quad + a_r(x, y) a_i(x, y) \cos((\omega_r + \omega_i)t + (\phi_r(x, y) + \phi_i(x, y))) \\ &\quad + a_r(x, y) a_i(x, y) \cos((\omega_r - \omega_i)t + (\phi_r(x, y) - \phi_i(x, y))) \end{aligned} \quad (2)$$

where $\omega = 2\pi f$. When this resultant beam is detected by the MLC, temporally varying components, where ω is ω_r , ω_i and $\omega_r + \omega_i$, are either not detected or filtered out. To simplify the detected signal equation, all frequency independent components are described by

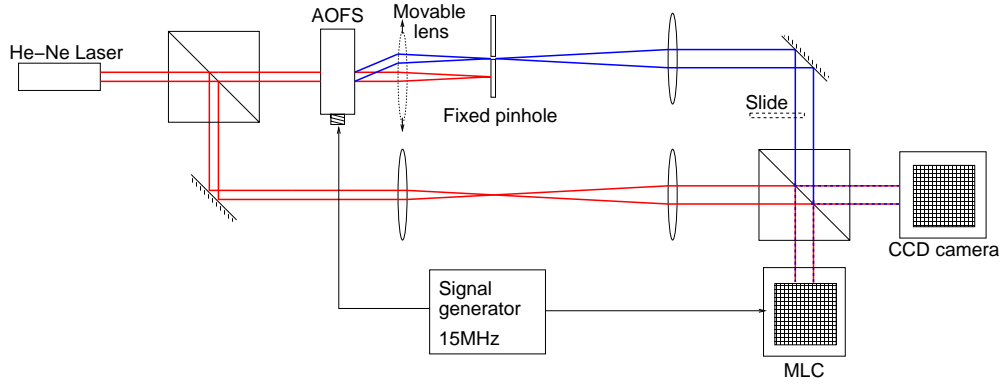


Fig. 1. Modified Mach-Zehnder heterodyne interferometer. The interferometer uses a fixed spatial filter/pinhole and a movable lens so that it can switch between homodyne and heterodyne modes while preserving the interferogram. In heterodyne mode the Bragg cell (AOFS) shifts the frequency of one arm of the interferometer resulting in a modulated interferogram at the detectors. The CCD camera cannot detect the high frequency modulation (15 MHz) and so captures just the DC. The MLC can detect the frequency modulated component (as well as the DC component) by electronically mixing the received signal at each pixel with in-phase (I) and quadrature (Q) signals. These I and Q signals can be derived from the signal generator that drives the Bragg cell.

$I_{dc}(x, y) = 1/2a_r(x, y)^2 + 1/2a_i(x, y)^2$, the amplitude of the temporally varying component is described by $A(x, y) = a_r(x, y)a_i(x, y)$ and the differences in beam frequency and phase are described by $\omega_d = \omega_r - \omega_i$ and $\phi_d = \phi_r - \phi_i$ respectively,

$$I(x, y, t) = I_{dc}(x, y) + A(x, y) \cos(\omega_d t + \phi_d(x, y)) \quad (3)$$

The phase difference, ϕ_d , will remain constant if the optical path length difference between the two beams remain unchanged. This is usually the value of interest and will change if the optical path length difference changes (e.g. by 2π for a shift of λ) or if a subject is introduced into the interferometer. For homodyne interference, $\omega_d = 0$, and all phase information is extracted from the intensity (Eq. (10)).

The prototype MLC detects $I(x, y, t)$ on the photodiode and extracts I_{dc} , $A(x, y)$ and $\phi_d(x, y)$ as V_{DC} , V_I and V_Q components using filters and quadrature demodulation. The modulated light camera can be used to output a widefield AC image using the interference pattern. Quadrature demodulation has been used before to output the phase information of a heterodyne interference pattern [7, 8]. The measured signal is mixed with an in-phase signal, I_{in} , and a quadrature signal, Q_{in} . The signals have the same frequency as the beam frequency difference, ω_d , the beat frequency. The difference in signals is a phase difference of 90° , hence

$$\begin{aligned} I_{in} &= B \cos(\omega_d t) \\ Q_{in} &= B \sin(\omega_d t) \end{aligned} \quad (4)$$

Mixing the measured signal with the in-phase and quadrature signal produces $I_{outp}(x, y, t)$ and $Q_{outp}(x, y, t)$,

$$\begin{aligned} I_{outp}(x, y, t) &= I_{dc}(x, y)B \cos(\omega_d t) + \frac{BA(x, y)}{2} [\cos(2\omega_d t + \phi_d(x, y)) + \cos(\phi_d(x, y))] \\ Q_{outp}(x, y, t) &= I_{dc}(x, y)B \sin(\omega_d t) + \frac{BA(x, y)}{2} [\sin(2\omega_d t + \phi_d(x, y)) + \sin(\phi_d(x, y))] \end{aligned} \quad (5)$$

The signals are mixed using Gilbert cells, which accurately multiply both inputs. A differential output is generated, denoted by $I_p(x,y)$ and $I_n(x,y)$ for the in-phase output, and $Q_p(x,y)$ and $Q_n(x,y)$ for the quadrature output. These signals are low pass filtered to remove any temporally varying components, to give

$$\begin{aligned} I_p(x,y) &= \frac{BA(x,y)}{2} \cos(\phi_d(x,y)) & I_n(x,y) &= -\frac{BA(x,y)}{2} \cos(\phi_d(x,y)) \\ Q_p(x,y) &= \frac{BA(x,y)}{2} \sin(\phi_d(x,y)) & Q_n(x,y) &= -\frac{BA(x,y)}{2} \sin(\phi_d(x,y)) \end{aligned} \quad (6)$$

The phase information can now be extracted, without any influence from the amplitude. To get the most information out of the data collected and reduce systematic error, the equation below, which makes use of all four differential outputs, is used,

$$\phi_d(x,y) = \arctan\left(\frac{Q_p(x,y) - Q_n(x,y)}{I_p(x,y) - I_n(x,y)}\right) = \arctan\left(\frac{Q_d(x,y)}{I_d(x,y)}\right) \quad (7)$$

An image can be created to show the AC phase as a value modulo 2π .

3. Modulated light camera

The prototype MLC was fabricated as a custom camera chip using a $0.35\ \mu\text{m}$ standard CMOS process. It has 32×32 pixels, with a fill factor of 16% and a pixel pitch of $115\ \mu\text{m}$. Previous implementations of the camera included a single test pixel [13] and use of the previous generation of the camera used for LIDAR purposes [14]. Other cameras developed by our group include a dual phase [15] and quad phase [16] synchronous light detectors, which are capable of quadrature demodulation at frequencies less than $1\ \text{MHz}$, and uses square wave inputs for demodulation, which could add distortion in the form of harmonics when compared with a system that uses sinusoidal inputs. Each pixel of the camera contains: a photodiode, transimpedance amplifier (TIA), a pair of analogue mixers and filters seen in Fig. 2a. Each pixel can demodulate the in-phase (I) and quadrature (Q) components of the received signal simultaneously. Each pixel is equipped with post mixer electronic filters. These remove unwanted high frequency components resulting from the mixers and provide some signal averaging. Their bandwidth is set to $1\ \text{kHz}$, which is approximately the maximum complete frame readout rate for the camera. The result is that each pixel produces DC voltages V_{DC} , V_I and V_Q . The amplitude of the signal (proportional to the intensity of the modulated component) is given by $|V_I + iV_Q|$ and the phase of the signal is given by $\arctan(V_Q/V_I)$. This phase is the phase difference between the object and reference beams in the interferometer.

The TIA uses a modified log pixel [9] in order to provide high gain in a small physical area. Normally such a log pixel produces a log response to intensity. The TIA has been modified to linearise the response in order to remove unwanted harmonics and distortion of the phase measurement. The details of the electronics will be published at a later date. The MLC pixels also simultaneously report the DC intensity. The experimental setup shown in Fig. 1 is used to capture the switching between the homodyne and heterodyne patterns, seen in Fig. 5 and Fig. 6 respectively.

The RF response of the camera largely determines the choice of modulation frequency used, shown in Fig. 2b. The figure, which is normalised using the mean of the values from the maximum and $-3\ \text{dBm}$ below, shows that the variation in amplitude drops off after the $15\ \text{MHz}$ point. Figure 3 shows the output phase relative to the input phase, produced by the incident light. The error between the input and measured phase is shown in Fig. 4 as a solid line. The maximum error present at $15\ \text{MHz}$ with 120 averages is $\pm 0.1116\ \text{radians}$ once results have been offset, giving a maximum error in phase accuracy of 1.8%. It is possible to see that there is

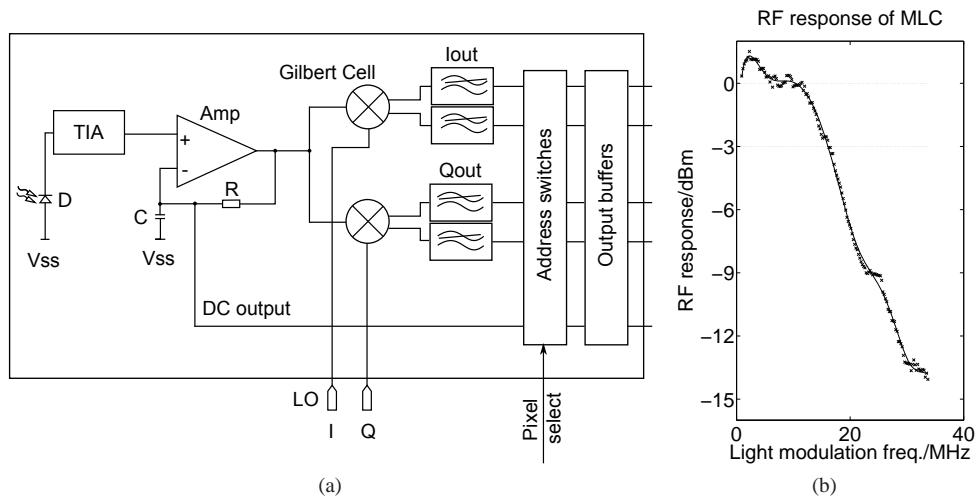


Fig. 2. (a) Schematic of MLC pixel. The light is detected on a photodiode. The resultant photocurrent is converted to a voltage and amplified using a compact high speed and high gain transimpedance amplifier. The signal is then mixed down to DC voltages in the I and Q mixers and electronically low pass filtered before being passed to the pixel read out circuitry. The pixels also contains a DC output and some pixels in the array contain raw AC outputs (RFout). (b) Frequency response of the MLC pixel. This is the response to modulated light at the photodiode, measured at RFout.

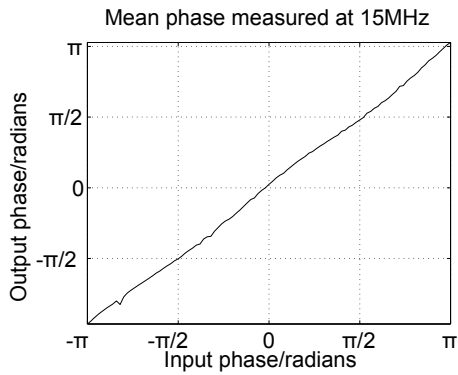


Fig. 3. Measured phase at 15MHz

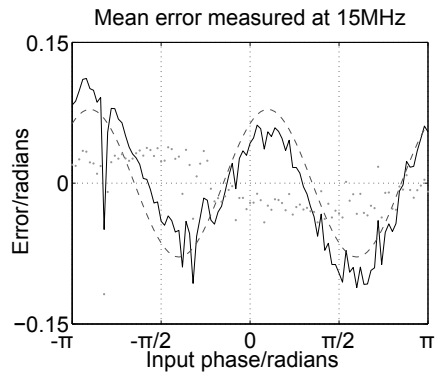


Fig. 4. Error in phase at 15MHz

a systematic error present in the mean error measured. This residual error could be the result of a slight imbalance between the mixers or possibly from an imbalance in the reference signals (I and Q input), in phase (not exactly 90° difference) or amplitude. The error appears to follow a sine function (dashed line in Fig. 4). Using this as a reference, the error can be eliminated further, with an estimated maximum phase error (not including one anomalous result) of ± 0.041 radians ($\pm 2.389^\circ$), shown in Fig. 4 as dots. This will be improved on in future versions.

4. Experimental method

The light source used is a He-Ne 633 nm 6.5 mW laser shown in Fig. 1, with a 1 mm diameter beam. The beam is split and in one arm it passes through a Bragg cell driven at a frequency of 15 MHz . The Bragg cell produces several orders of diffraction and in this experiment the 0-order, which is not frequency shifted, and the 1st order, which is shifted by 15 MHz , can be selected by adjusting the movable lens to pass the required order through the fixed pinhole. The interferometer can be changed from homodyne to heterodyne modes without changing the spatial phase relationship, ϕ_d , between the object and reference beams.

Because the pinhole has a fixed position, a large amount of power is lost through the Bragg cell which is not operating at its optimal frequency (40 MHz). After spatial filtering and frequency shifting the optical power of the subject beam is measured to be 0.76 Wm^{-2} , whilst the reference beam was measured to have 42.03 Wm^{-2} of power. The position of the collimating lenses in the arms of the interferometer were adjusted to produce a collimated reference beam and a weakly spherical object beam at the cameras. The MLC was controlled using a data acquisition card (12-bit DAC) under computer control. The data is read using gray code to minimise read errors due to switching. A signal generator was used to drive the Bragg cell, through an amplifier, and provide the I and Q signals to the camera. Using this arrangement, simple models can be generated of interferograms and subjects can be inserted into the interferometer for analysis.

5. Results

The images captured using the MLC are of a spherical wave interfering with a uniform wave. This arrangement was chosen as it is a simple interference to model and set up experimentally. Equations (8) and (9) describe the phase of a uniform wave, $\phi_p(x,y)$, and a spherical wave, $\phi_s(x,y)$ respectively;

$$\phi_p(x,y) = \frac{2\pi}{\lambda}(x\sin(\theta_x) + y\sin(\theta_y)) \quad (8)$$

$$\phi_s(x,y) = \frac{2\pi}{\lambda}(x^2 + y^2 + F^2)^{\frac{1}{2}} \quad (9)$$

where F is the focal point of the exit lens. As mentioned, the setup allows switching between heterodyne and homodyne interference mode. The spatial filter allows interference between the reference beam and the 0^{th} or the 1^{st} order beam from the Bragg cell. Figure 5 shows a homodyne fringe pattern, slightly off the centre circle, showing more fringes. The phase image seen in Fig. 6 shows the heterodyne interference pattern. It is clear that the same fringe pattern is captured in heterodyne mode as in homodyne mode. The centre circle of the fringe pattern is in the same place, with the same outer rings visible.

To check on the performance of the MLC the measured phase was compared with the phase predicted from Eqs. (8) and (9). Initial experiments are conducted by shifting the exit lens of the reference arm by 5 mm , creating a spherical wave. The calculated and measured phase in degrees are shown in Fig. 7 and Fig. 8 respectively. The difference between the images can be seen in Fig. 9. The difference image is also presented modulo 2π , seen in Fig. 10. The patterns are almost identical with a slight angular variation and phase unevenness.

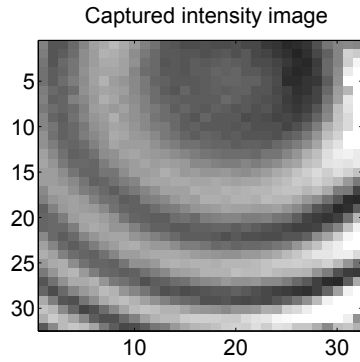


Fig. 5. DC homodyne pattern.

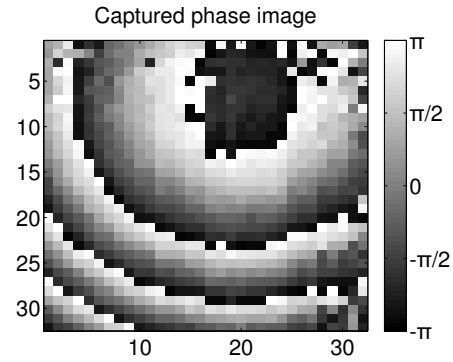


Fig. 6. Phase heterodyne pattern.

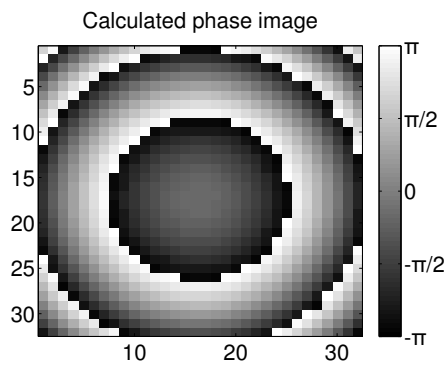


Fig. 7. Theoretical phase image.

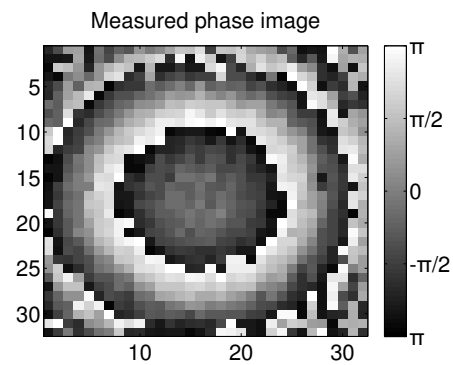


Fig. 8. Captured phase image.

The phase information captured is presented as a value modulo 2π due to the arctan operation. The pattern can be unwrapped beyond the 2π range computationally using the same reference point. Using the same spherical on uniform wave experiment, Fig. 11a and Fig. 11b shows the theoretical wrapped and unwrapped calculated phase image respectively, Fig. 11c shows the measured phase image and Fig. 11d is the unwrapped image of the captured phase image.

To perform an interferometry experiment, a microscope slide was placed over half the reference arm beam, which will change the phase, $\phi_r(x, y)$, across half the image. The phase shift induced by the microscope slide varies and the MLC is used to determine the phase. Figure 12a shows the phase image before the slide is introduced (control image), with Fig. 12b showing the difference between another image without a slide present after being unwrapped. The phase across the camera should stay constant if the fringe pattern does not change.

The slide covers the left half of the MLC (x-axis pixels approximately less than 16), with the right half of the MLC (x-axis pixels approximately more than 18) being uncovered. Figure 12c shows the phase image with the slide placed in the setup and Fig. 12d shows the difference image between the slide and control image. The right side of the image is constant as in Fig. 12b meaning that this side has the same fringe pattern as the control image and therefore no slide is present. The phase on the the left side of the image has changed in Fig. 12d as is consistent with the introduction of the slide.

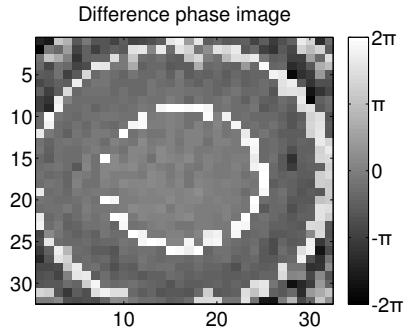


Fig. 9. Image of difference between theoretical and captured.

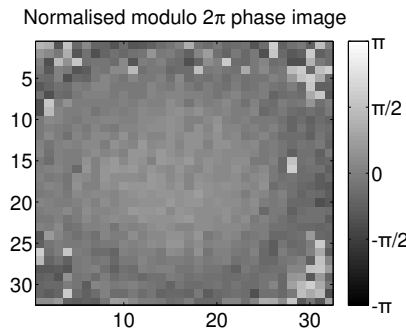


Fig. 10. Modulo 2π of difference image.

6. Discussion and conclusion

Interferometry is used in many different fields to measure optical path length difference of two beams of light, a subject and a reference beam. A change due to an environmental effect or object in path of the subject beam will change the optical path length. The phase of the light at the point of interference will differ. A phase change of 2π is the equivalent of a change in path length of one wavelength. This is detected using a photo-detector and calculations are conducted to translate path length change to a more useful measurement.

In homodyne interferometers, the phase change due to a path length change results in a fringe pattern that has static intensity, as shown in Fig. 5. An equation to determine the phase difference in homodyne interferometry, Eq. (3) can be used if $f_d = 0$. The homodyne interferometry mode intensity, $I_{\text{homo}}(x, y)$, is equal to,

$$I_{\text{homo}}(x, y) = I_{dc}(x, y) + A(x, y) \cos(\phi_d(x, y)) \quad (10)$$

The phase, $\phi_d(x, y)$, can be determined by removing any constant intensity and multiplying factor. This can be done by using filtering techniques and the phase can be determined by calibrating the system using phase shifting. However, this type of interferometry is susceptible to background optical interference as well as from mechanical interference.

Heterodyne interferometers use light that has different frequencies. The intensity due to the superposition of the two beams will change sinusoidally; the light is amplitude modulated. As the initial phase shift is different at various points in the interference fringe pattern, measuring

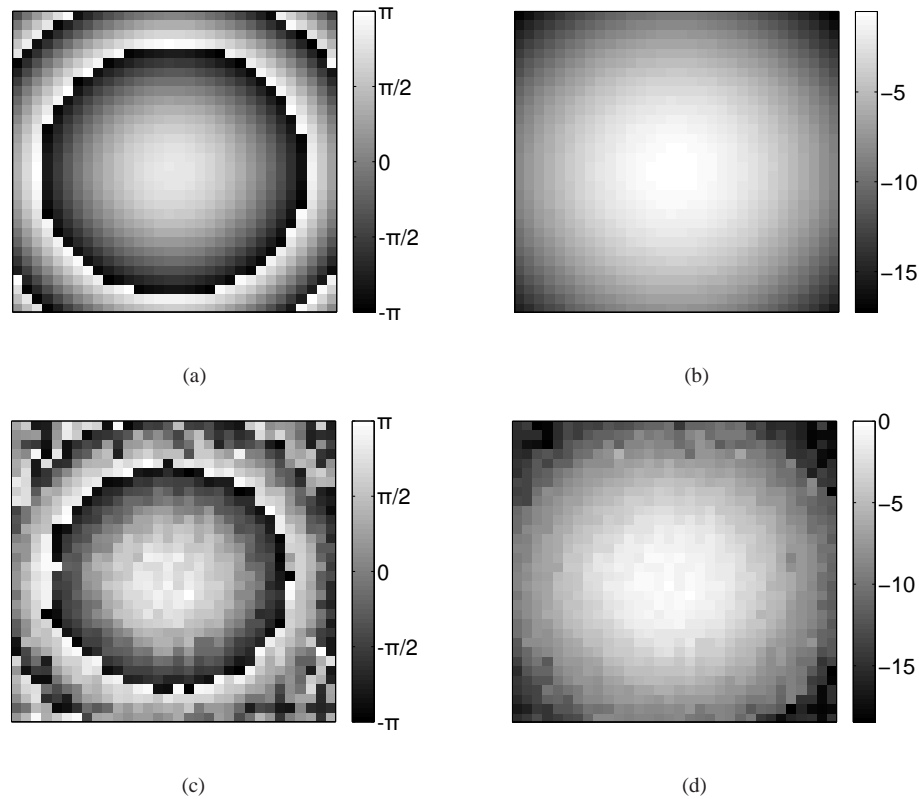


Fig. 11. Phase images (top) (a) wrapped and (b) unwrapped theoretical images of the fringe pattern, (bottom) (c) measured fringe pattern (d) unwrapped measured fringe pattern.

the phase in the modulated signal will reveal the fringe pattern, as can be seen in Fig. 6.

In this paper we have demonstrated a widefield heterodyne interferometer using a prototype MLC. This camera can demodulate the AC component in a heterodyne image. The camera measures the the DC intensity, AC amplitude and optical phase directly with no need for further processing or phase stepping.

Widefield heterodyne interferometry is demonstrated using a novel Mach-Zehnder interferometer. The system presented captures fringe patterns generated by a spherical wave on uniform wave interference. The phase image can be unwrapped computationally, making phase comparisons beyond the 2π range possible. This interferometer allows switching from heterodyne to homodyne modes without changing the interferogram which facilitates a direct comparison with the homodyne interferogram. Heterodyne interferogram are shown and compared with a theory and a measurement of the phase from an object is demonstrated.

This prototype system can achieve a phase measurement accuracy of $\pm 6.6^\circ$ at a light power of 8nW per pixel without systematic phase correction. In addition to random electronic noise, the error in phase follows a sine wave (as can be seen in Fig. 4), which could be attributed to the reference signals, I and Q, not being completely 90° out of phase or amplitude matched. This can be eliminated by using a better calibrated signal source (hardware) or computationally after capture (software). The noise can also be reduced by increasing the optical power. The modulation frequency also contributes to the SNR, as indicated by Fig. 2b. The lower frequencies have a much larger response. The choice of using 15MHz as the modulation frequency comes

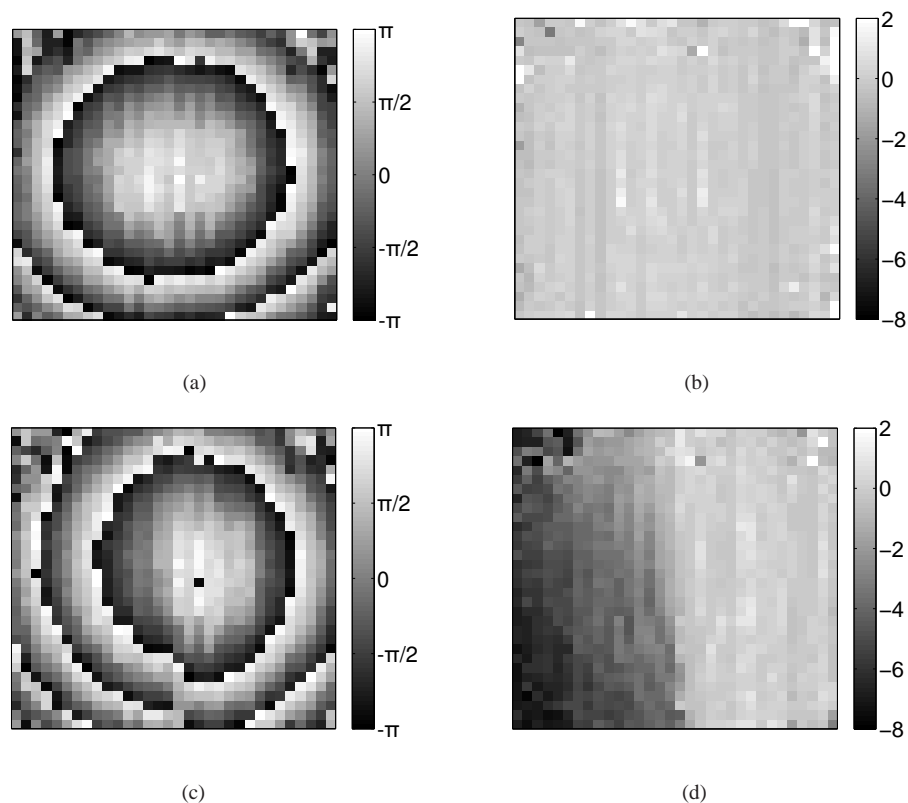


Fig. 12. (left) Heterodyne fringe patterns (a) without a slide, (c) with a slide. (right) Difference fringe pattern after unwrapping (b) without slide, (d) with a slide.

from high RF response and the being able to reliably drive the Bragg cell.

The camera presented in this paper is a custom CMOS modulated light camera. It has a 32×32 pixel array. The camera has an operating bandwidth from 100kHz to 45MHz with a minimum light power of around 1.5nW per pixel. The camera saturates at $1.3\text{ }\mu\text{W}$ per pixel (the amount of light power used for this paper was about 90nW pixel). Whilst other works presented have shown widefield heterodyne images, they were working with modulation frequencies between 10kHz to 25kHz [10, 11]. Using an integrated camera has many uses for the field of interferometry. Integrating the interferometer and the capturing device as a subsystem to provide real time information can be used as part of medical systems, in industrial analysis as well as subject characterisation.

At present, the electronic reference used for demodulation in the MLC is derived from the signal that produces the modulation (i.e. the signal used in the Bragg cell). However, we conjecture that deriving this from the optical signal received (by using the RF output of a single pixel) would allow the effects of vibration (piston phase) to be removed and open the possibility for creating an ultrastable configuration and even for deriving the object and reference beams from separate (frequency stabilised) lasers.